Available online at www.sciencedirect.com

ScienceDirect

Procedia Engineering 2 (2010) 129–138

Procedia Engineering

www.elsevier.com/locate/procedia

Fatigue 2010

Fatigue performance of resistance spot welds in three sheet stack-ups

Hong-Tae Kang[a,*], Ilaria Accorsi[b], Bipin Patel[b], Eric Pakalnins[b]

[a]*University of Michigan-Dearborn, 4901 Evergreen Road, Dearborn, Michigan 48128, USA*
[b]*Chrysler LLC.,800 Chrysler Drive, Auburn Hills, Michigan 48326, USA*

Received 1 March 2010; revised 10 March 2010; accepted 15 March 2010

Abstract

This paper describes the fatigue characteristics of spot welds for three equal thickness sheet stack-ups of a Dual Phase (DP600) welded to itself and a Mild steel welded to itself under tensile shear loading. The experiments were designed to investigate the effects of electrode tip geometries, surface indentation levels, and base metal strengths on fatigue life of the tensile shear spot welds. The electrode tip geometries were B-nose for DP600 and Mild steel and E-nose for DP600. Surface indentation levels were 10%, 30% and 50% of the sheet thickness. To obtain the goal, geometric factors were precisely controlled, especially the diameters of spot welds. Welding schedules varied to obtain proper surface indentation levels while keeping the same weld sizes for the different materials and electrode geometries. The fatigue test results showed scatter in the plot of the maximum applied loads versus cycles to failure of spot welds due to weld sizes and base metal strengths. Thus, a normalized structural stress parameter was proposed and correlated well to the fatigue test result

Keywords: Fatigue life; Spot weld; High strength steels; Hardness

1. Introduction

The automotive industry is currently facing enormous challenges to develop more fuel efficient vehicles due to stringent government regulation and high gas prices. To achieve the goal in vehicle structure design, lightweight materials such as aluminium alloys, magnesium alloys, and composite materials are used more frequently. However, these lightweight materials are expensive compared to sheet steels. Thus, thinner advanced high strength steels (AHSS) are used to substitute for thicker mild steels and high strength steels components to reduce weight of the vehicle structure.

Electrical resistance spot welding is a widely used technique in the automotive industry to join sheet steels for uni-body and body on frame structures. The integrity of the uni-body structure relies on the strength of spot welds. The typical car uni-body structure contains more than 3000 spot welds to join the sheet steels [1]. Geometric shapes of the spot welds subjected to various loads applied on the spot welds induce stress concentration that can lead to fatigue crack initiation at periphery of the spot weld. The cracks can degrade structural integrity and increase noise and vibration of the vehicle structure. Therefore, the fatigue performance of the spot welds should be investigated in vehicle structure design.

Many researchers [1~10] studied the effects of nugget diameter, sheet thickness, specimen width, and base metal properties on the fatigue performance of spot welds. They also studied the effects of loading conditions with tensile

1877-7058
doi:10.1016/j.proeng.2010.03.014

shear, coach peel, and cross tension specimens. The studies showed that fatigue strength of spot welds generally depended on the loading types and geometric dimensions of the spot welds. The studies also confirmed that the fatigue strength of spot welds decreased as the applied load range increased, but increased as weld size increased [1~10].

Numerous previous researchers [9~21] proposed analytical and/or empirical models to predict the fatigue life of spot welds. Some researchers [9,10] developed empirical relationship among geometric factors, loading conditions, and the number of cycles to failure. On the other hand, some researchers [22] used a numerical method to predict fatigue strength. Most of previous studies were based on spot welded joints of two sheets. However, vehicle structures have a very large number of spot welds joining three sheets.

This study investigated the fatigue characteristics of spot welds fabricated with three equal thickness sheet stack-ups of DP600 welded to itself and a mild steel welded to itself using two different welding electrode tip geometries and three different indentation levels. Three equal sheet thickness specimens were used to facilitate consistent surface indentation and weld size at the tested faying surface.

This paper described the effect of electrode tip geometries, indentation levels, and material properties of base metals on fatigue strength of spot welds fabricated with three sheet stack-ups. This study also tried to correlate the fatigue test results with fatigue damage parameters proposed in [4, 12, 17, and 19].

Nomenclature

TS10BDP	Tensile Shear specimens of DP600 welded with B-nose tip achieving 10% surface indentation
TS30BDP	Tensile Shear specimens of DP600 welded with B-nose tip achieving 30% surface indentation
TS50BDP	Tensile Shear specimens of DP600 welded with B-nose tip achieving 50% surface indentation
TS10EDP	Tensile Shear specimens of DP600 welded with E-nose tip achieving 10% surface indentation
TS30EDP	Tensile Shear specimens of DP600 welded with E-nose tip achieving 30% surface indentation
TS50EDP	Tensile Shear specimens of DP600 welded with E-nose tip achieving 50% surface indentation
TS10BMS	Tensile Shear specimens of Mild Steel welded with B-nose tip achieving 10% surface indentation
TS30BMS	Tensile Shear specimens of Mild Steel welded with B-nose tip achieving 30% surface indentation
TS50BMS	Tensile Shear specimens of Mild Steel welded with B-nose tip achieving 50% surface indentation
$\sigma_{eq}(\theta)$	Equivalent structural stress along circumference of spot weld
$\sigma_{\max}(F_x)$	Maximum stress induced by x-direction force (F_x)
$\sigma_{\max}(F_y)$	Maximum stress induced by y-direction force (F_y)
$\sigma(F_z)$	Stress induced by z-direction force (F_z)
$\sigma_{\max}(M_x)$	Maximum stress induced by moment about x-axis (M_x)
$\sigma_{\max}(M_y)$	Maximum stress induced by moment about y-axis (M_y)
κ	A material dependent geometry factor
d	Nugget diameter
t	Sheet thickness
σ_{meq}	Maximum equivalent structural stress
σ_y	Yield strength of material
S_{norm}	Normalized Rupp and co-workers' structural stress

2. Materials, Specimens and Weld Procedures

This study used two different materials, DP600 and a mild steel, to fabricate three sheet stack-ups of tensile shear specimens to characterize fatigue performance of spot welds. The chemical compositions of the sheet steels are shown in Table 1. The thickness of DP600 coupons was 1.64 mm and that of the mild steel was 1.57 mm. In all cases, the face diameter of the electrode tips was 4.8 mm and the target weld size at the tested faying surface was 5.5 mm +/- 0.5mm. The specimens from each material had three indentation levels, 10%, 30% and 50%. The effect of electrode tip geometry (B-nose and E-nose) was compared on DP specimens, and the effect of material strength (DP 600 and mild steel) was compared on samples made with the B-nose electrode tip. The shapes of the electrodes are shown in Figure 1. Coupon shapes and dimensions of the TS specimens are shown in Figure 2. The indentation was determined based on the anticipated height from a reference line drawn between point A and Point B to the depth of the crater area as shown in Figure 3. This height was one half the differences in Point A and Point B's heights.

Table 1. Chemical Composition of the Materials in Weight Percentage

	C	Si	Mn	P	S	Cr	Mo	Ni
Mild Steel	<0.001	0.001	0.077	0.008	0.012	0.023	0.004	0.013
DP600	0.0759	0.01	1.894	0.014	0.006	0.181	0.175	0.014
	Al	Cu	Nb/Cb	Ti	V	Sn	Fe	B
Mild Steel	0.0264	0.032	0.01	0.0443	<0.001	0.001	99.748	<0.000
DP600	0.0427	0.031	0.006	0.0025	0.002	0.003	97.542	<0.000

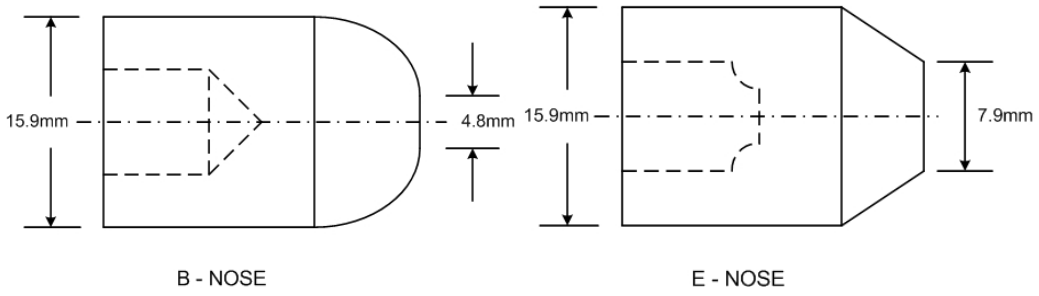

Fig. 1. Shapes of the electrode tip for B-Nose and E-Nose.

Prior to welding the test specimens, the electrodes were stabilized using a setup weld schedule with 4.23 kN of weld force, 24 cycles of weld time (3 pulses of 8 cycles, 2 cycle cool time), 5 cycles of hold time, and 10.5 kA of weld current. The targeted weld size and indentation levels were obtained by adjusting the welding schedule parameters. For subsequent coupon pairs, the weld current, weld time, and/or the weld force were adjusted as necessary in order to obtain the target weld size (5.5 mm ±0.5) and required indentation percentage. Once the desired minimum weld size and indentation percentage was attained, the weld parameters were maintained to fabricate tensile shear specimens for the specific indentation level. Every sixth specimen was destructively peel tested and the targeted weld size verified. For all specimens fabricated, the actual current, indent depth, and occurrence of expulsion were recorded. The weld parameters for all specimen fabrication and resulting weld sizes and indentation levels are shown in Table 2.

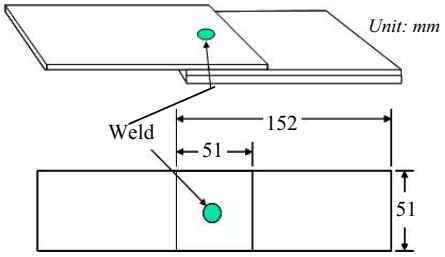

Fig. 2. Geometry and dimensions of the specimen.

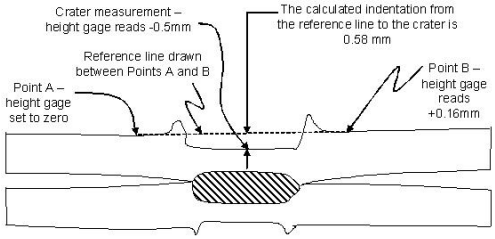

Fig. 3. Nugget indentation and distortion.

It was observed that high weld force and/or high weld time increased the indentation levels in DP600 and the mild steel as shown in Table 2. Different weld schedules had to be used for the different cap types. Weld sizes were consistent for all specimens except 10% indentation of DP600 E-Nose. The actual indentation levels were very close to the target indentation for all specimens.

Table 2. Weld Parameters and resulting Weld Diameters and Indentation Levels

		DP600, B-Nose			DP600, E-Nose			Mild Steel, B-Nose		
Indentation Target, (%)		10	30	50	10	30	50	10	30	50
Weld Current, (kA)		8.2	8.7	7.9	10.1	7.4	7.9	8.8	9.8	10.9
Weld Time, (Cycles)		17	18	60	12	52	60	20	21*	27**
Weld Force, (kN)		3.6	7.1	11.1	4.2	7.6	11.12	2.5	4.2	6.7
Button Size, (mm)	AVG	5.5	5.7	5.8	5.3	5.7	5.7	5.8	5.8	5.5
	STDEV	0.195	0.172	0.129	0.293	0.120	0.112	0.362	0.223	0.259
Actual Indentation, (%)	AVG	12.4	26.8	47.0	12.0	31.6	49.2	13.0	30.8	49.3
	STDEV	0.694	0.734	0.449	1.089	1.193	0.892	1.028	0.955	1.246
Notes: "" – 3 pulses of 7 cycles with 1 cycle cool between pulses & "**" – 3 pulses of 9 cycles with 2 cycles cool between pulses.*										

Micro-hardness tests were also performed on nine different specimens. The hardness measurements were made at equal distances (0.381 mm) on a diagonal line from the base material, through the heat affected zone (HAZ) and weld nugget, and then through the HAZ back into base material as shown in Figure 4. From the observations, the nugget material was harder than the base metal for all specimens tested. The increment of the hardness in the nugget was much higher with DP600 than with mild steel. It was also observed that the hardness value dropped in the Heat Affected Zone (HAZ) of DP600, but that was not observed with the HAZ of mild steel.

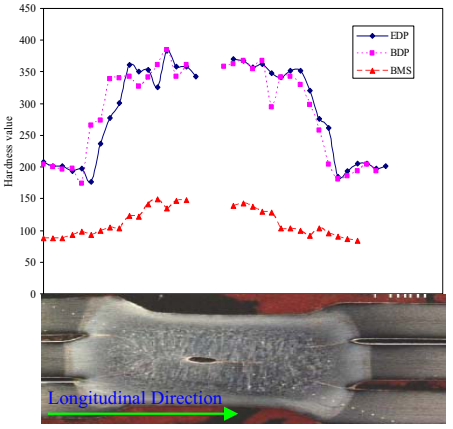

Fig. 4. Micro-hardness profiles around fusion zone for DP600 and mild steel.

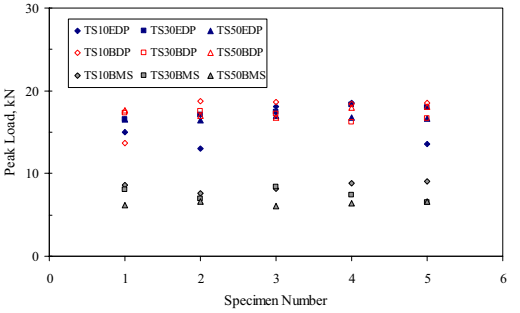

Fig. 5. Peak loads for electrode tip types and indentation combinations.

3. Static and Fatigue Strength Tests of Spot Welds

3.1. Static Strength of Spot Welds

Static strength tests for tensile shear spot welds were initially conducted for the three sheet stack-ups of DP600 and mild steel. The effect of surface indentation combinations made using both types of electrode tips and material on static weld strength was identified. Five replicates were tested for each electrode tip geometry and indentation combination, and the averaged static weld strengths were used to approximate the maximum single cycle load capability. Then, 40 and 60 percent of these maximum values were selected as the load levels for the initial fatigue tests. The peak loads of static weld strength are plotted in Figure 5. DP600 specimens were stronger than mild steel specimens regardless of indentation levels. No significant effect of indentation percentage on static weld strength was observed. The static strength for 10% indentation of DP600 with E-nose tip (TS10EDP) is lower compared to other DP600 specimens. However, this is believed to be the result of a smaller weld size as documented in Table 2.

3.2. Fatigue Strength of Spot Welds

Each specimen was tested in tensile shear fatigue loading at room temperature at a frequency of 10Hz with sine wave load application at R=0.01. The failure criterion for fatigue tests was that specimens were completely separated in two pieces. The runout cycle was 1,000,000 in the fatigue tests.

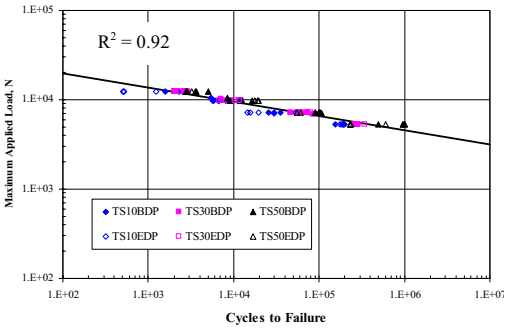

Fig. 6. Max. applied load vs. fatigue life for DP600.

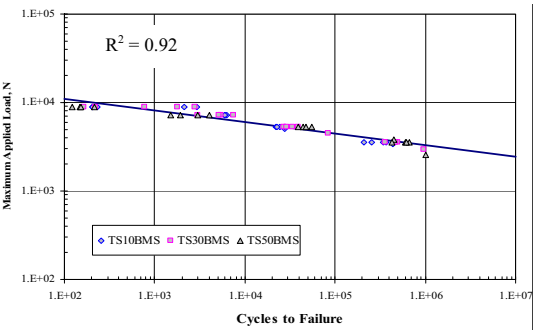

Fig. 7. Max. applied load vs. fatigue life for Mild steel.

Figure 6 shows the effect of electrode tip geometry (B-nose and E-nose) and indentation levels on fatigue strength of spot welds for DP600 tensile shear specimens. All data were well collapsed along the best-fit line. When plotting the results of the fatigue life for DP 600 samples made using the B electrode and E electrode cap, it can be seen that there is a slight improvement in fatigue life with deeper indentations. Since the correlation coefficient (R^2) is equal to 0.92, from practical point of view this dependency is considered negligible. The fatigue life of TS10EDP specimens was shorter than other samples due to smaller weld size as documented in Table 2. For mild steel specimens, scatter was observed at the highest applied load cases as shown in Figure 7.

The fatigue test results of three sheet stack-up spot welds for DP600 and the mild steel are shown in Figure 8. The correlation coefficient (R^2) was only 0.62 and clear separation was observed between DP600 and mild steel fatigue results. This means that material strength significantly affect the fatigue strength of spot welds fabricated with three sheet stack-ups. On the other hand, again weld indentation levels did not show a strong relationship to the fatigue strength of the spot welds tested. In the shorter fatigue life regions, more scatter was observed as shown in Figure 8.

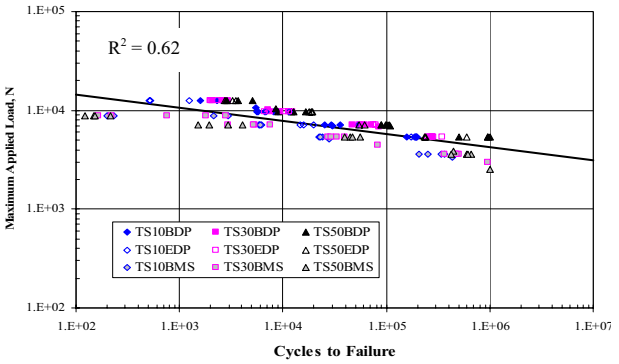

Fig. 8. Max. applied load vs. fatigue life for all specimens tested.

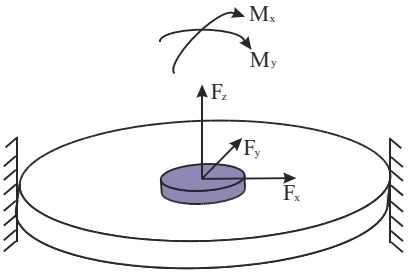

Fig. 9. Forces and moments at a spot weld [1].

4. Correlations for Fatigue Results of Spot Welds

Scatter is the nature of fatigue test results and comes from various origins including specimen geometric factors, welding parameters, and base metal properties. Thus, numerous researchers [9~21] had developed various fatigue damage calculation methods to correlate the fatigue test results of spot welds. Most widely accepted damage calculation method for spot welds is the structural stress approach proposed by Rupp *et al*. [17].

They observed that spot welded connections experienced considerable local plastic deformation during the first load cycle. Therefore, the linear elastic finite element method cannot calculate the exact stresses at spot welds, and the linear notch-root stresses or stress intensities cannot be a good damage parameter for fatigue strength of spot welds. They proposed a fatigue damage parameter based on local structural stresses calculated from the cross-sectional forces and moments at a spot weld using beam, sheet, and plate theory. To determine the forces and moments at the spot welded joints, a stiff beam element was used in the finite element model to connect sheet metals. The length of this beam element was one-half of the total thickness of the two sheets joined [17].

The equivalent stresses were calculated by combination and superposition of the local structural stresses, and as a function of angle θ around the circumference of the spot weld. Here, θ is the angle measured from a reference axis. Figure 9 shows the forces and moments at a spot weld. The equivalent stresses for cracking in the sheet are calculated using superposition of formulae for the plate subjected to central loading as below:

$$\sigma_{eq}(\theta) = -\sigma_{\max}(F_x)\cos\theta - \sigma_{\max}(F_y)\sin\theta + \sigma(F_z) + \sigma_{\max}(M_x)\sin\theta - \sigma_{\max}(M_y)\cos\theta \quad (1)$$

where: $\sigma_{\max}(F_x) = F_x / \pi dt$, (2)

$\sigma_{\max}(F_y) = F_y / \pi dt$, (3)

$\sigma(F_z) = \kappa(1.744 F_z / t^2)$ for $F_z > 0$, (4)

$\sigma(F_z) = 0$ for $F_z \le 0$, (5)

$\sigma_{\max}(M_x) = \kappa(1.872 M_x / dt^2)$, (6)

$\sigma_{\max}(M_y) = \kappa(1.872 M_y / dt^2)$, (7)

$\kappa = 0.6\sqrt{t}$. (8)

The parameter κ is a material dependent geometry factor applied to the stress terms calculated from the bending moment. It effectively reduces the sensitivity of these stress terms to the sheet thickness.

This study used Rupp and co-workers' structural stress approach to correlate the fatigue results of spot welds. The maximum structural stress (σ_{meq}) was calculated at each specimen subjected to maximum applied load:

$$\sigma_{meq} = \max[\sigma_{eq}(\theta)] \quad (9)$$

To obtain forces and moments at spot welds, finite element analysis was conducted. In the finite element model, spot weld and coupons were modelled with a rigid beam element and shell elements, respectively. The tensile shear finite element model is shown in Figure 10. The maximum structural stress and fatigue life of the spot welds are plotted in Figure 11. The maximum structural stress at spot welds correlated a little better than the maximum applied loads did. However, it still shows noticeable scatter in Figure 11.

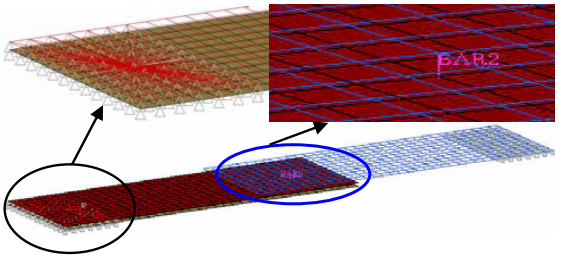

Fig. 10. Finite element model of a spot weld specimen.

Davidson's [4], Swellam's [12], and Zhang's [19] methods were also utilized to correlate the current fatigue results of spot welds. Here their equations are summarized and further information can be found in references sited in this paper. Davidson's equation [4] was expressed as

$$\Delta E = \frac{\Delta P \sqrt{\theta}}{t} \quad (10)$$

where ΔP is applied load range, t is sheet thickness, θ is nugget rotation, and ΔE is Davidson's parameter with unit of $\frac{N\sqrt{\deg ree}}{mm}$.

Swellam's K_i [12] was calculated as

$$K_i = K_{i_{\max}} \times (1 - R)^{b_o}, \quad (11)$$

$$K_{i_{\max}} = \frac{\left(\sqrt{K_{I_{\max}}^2 + \beta K_{II_{\max}}^2}\right)}{G}, \tag{12}$$

$$G = \left(\frac{9Wt^4}{4r^5} + \frac{Wt^2}{r^3}\right)^{1/2}, \tag{13}$$

where G is a geometry correction factor, r is nugget radius, t is sheet thickness, W is specimen width, R is load ratio, β is material constant, b_o is the load ratio effect, and $K_{i_{\max}}$ is the equivalent Mode I stress intensity factor taken at maximum applied load.

Zhang [19] proposed an equation for stress intensity factor for Mode I loading with applied load (P), nugget diameter (D), and sheet thickness (t) as below:

$$K_I = \frac{\sqrt{3}P}{2D\sqrt{t}} \tag{14}$$

The correlations were shown in Figures 12 - 14. However, no significant improvement was observed. Basically, the scatter in Figures 11 - 14 occurred between mild steel and DP600 but the parameters used in this study did not include the effect of base metal strength.

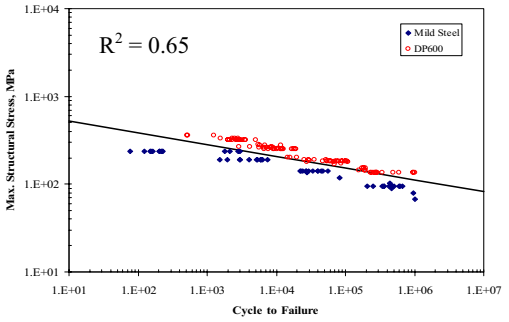

Fig. 11. Max. structural stress vs. fatigue life.

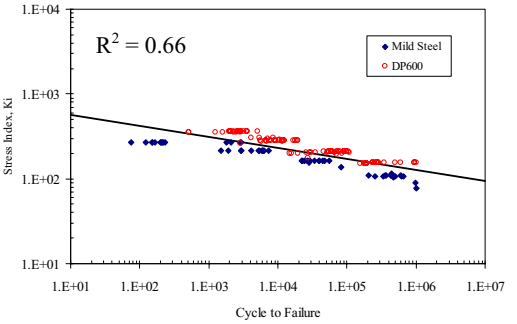

Fig. 12. Swellam's stress index vs. fatigue life.

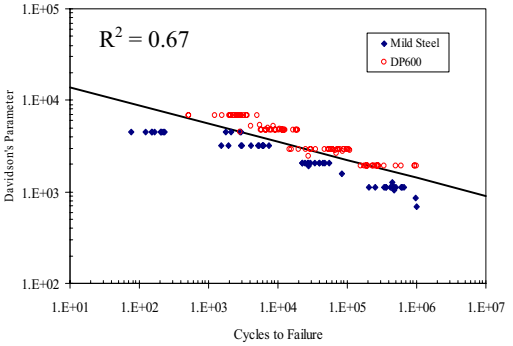

Fig. 13. Davidson's parameter vs. cycles to failure.

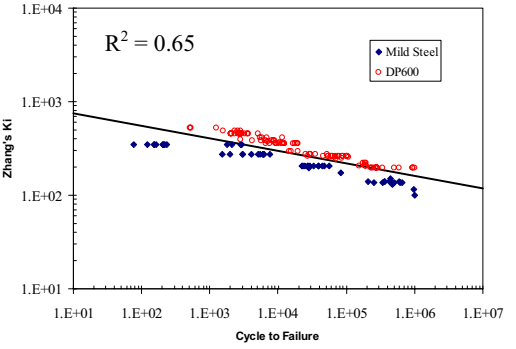

Fig. 14. Zhang's K_i vs. cycles to failure.

Thus, further investigations were conducted to reduce the scatter in the correlation between fatigue parameters and test results. The scatter could be coming from material strength since a clear separation exists between mild steel and DP600 in Figures 11 - 14. Therefore, the parameters were divided by a simple factor obtained from square

root of their yield strength values (no unit) of the base metals. This simple correlation factor between fatigue test results of DP600 and mild steel can be presented as the following Equations:

$$Y = \sqrt{\sigma_y} \tag{15}$$

$$S_M = \frac{\sigma_{meq}}{Y} \tag{16}$$

$$(K_i)_M = \frac{K_i}{Y} \tag{17}$$

The yield strength of the mild steel was 173 MPa and that of DP600 was 353 MPa. The modified maximum structural stress (S_M) and maximum stress intensity factor ($(K_i)_M$) were well correlated with current fatigue test results of spot welds for mild steel and DP600 as shown in Figure 15 and Figure 16, respectively.

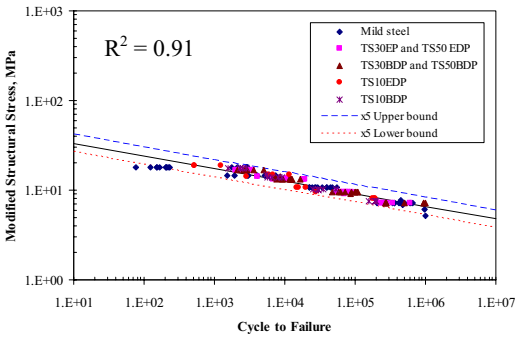

Fig. 15. Modified structural stress vs. cycles to failure.

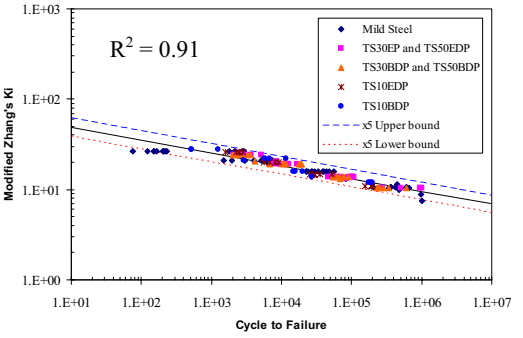

Fig. 16. Modified Zhang's K_i vs. cycles to failure.

5. Summary and Conclusions

Fatigue strength tests were conducted for tensile shear spot welds with three sheet stack-ups of DP600 and a mild steel. The specimens also included varying surface indentation levels as 10%, 30% and 50%. The DP600 specimens were also welded with E-nose and B-nose electrode tips to investigate the effect of electrode types on spot weld fatigue strength. However, only the B-nose electrode tip was used to weld the mild steel. The plot for maximum applied load versus cycles to failure of spot welds showed significant scatter due to material strengths. To reduce the scatter, a normalized structural stress parameter was introduced. From this study, the following conclusions can be drawn:

1. The electrode tip types (B-nose and E-nose) did not affect fatigue strength of spot welds for three sheet stack-ups of DP600.
2. The effect of surface indentation levels on fatigue strength of spot welds was negligible for DP600 and not existent in Mild Steel.
3. Fatigue strength of DP600 was higher than that of mild steel for resistance spot welds in the equal thickness three sheet stack-ups.
4. The plot for maximum applied load versus cycles to failure of spot welds showed significant scatter between DP600 and the mild steel. Swellam's, Davidson's, Zhang's and Rupp and co-workers' fatigue damage calculation methods could not reduce the scatter levels since those parameters only took in consideration specimen geometric factors.
5. The modified Zhang's and Rupp and co-workers' methods divided by a correlation factor obtained from square root of material's yield strength correlated well with the fatigue test results of DP600 and mild steel.

Acknowledgements

The authors are very thankful to Tom Morrissett, Mike Soter, and Don Maatz of RoMan Engineering Services Inc. for fabricating specimens, conducting tests, and providing some figures.

References

[1] Kang, H., Barkey, M. E., and Lee, Y. (2000) Evaluation of Multiaxial Spot Weld Fatigue Parameters for Proportional Loading, *Int. J. Fatigue* 22, 691-702.

[2] Orts, D.H. (1981) Fatigue Strength of Spot Welded Joints in a HSLA Steel, *SAE Technical Paper No. 810355*.

[3] Wilson, R.B. and Fine, T.E. (1981) Fatigue Behavior of Spot Welded High Strength Steel Joints, *SAE Technical Paper No. 810354*.

[4] Davidson, J. A. (1983) A Review of the Fatigue Properties of Spot-Welded Sheet Steels, *SAE Technical Paper No. 830033*.

[5] Jung, W.W., Jang, P.K., and Kang, S.S. (1996) Fatigue Failure and Reinforcing Method of Spot Welded Area at the Stage of Vehicle Development, *SAE Technical Paper No. 960553*.

[6] Bonnen, J., Agrawal, H., Amaya, M., Iyengar, R., Kang, H., Khosravaneh, A.K., Link, T., Shih, M., Walp, M., and Yan, B. (2007) Fatigue of Advanced High Strength Steel Spot Welds, SAE 2006 Transactions Journal of Materials & Manufacturing, 2006-01-0978.

[7] Kang, H., Iyengar, R., and Bonnen, J. (2007) Variability of Fatigue Strength of Spot Welded Specimens for Advanced and Traditional High Strength Steels, MS&T 2007, September 16~20, Detroit, MI.

[8] Rathbun, R.W., Matlock, D.K., and Speer, J.G. (2003) Fatigue Behavior of Spot Welded High-Strength Sheet Steels, *Welding Journal*, 207-S ~ 218-S.

[9] Lawrence, F.V., Jr., Wang, P.C., and Corten, H.T. (1983) An Empirical Method for Estimating the Fatigue Resistance of Tensile-Shear Spot-Welds, *SAE Technical Paper No. 830035*.

[10] Abe, H., Kataoka, S., and Satoh, T. (1986) Empirical Formula for Fatigue Strength of Single-Spot-Welded Joint Specimens under Tensile-Shear Repeated Load, *SAE Technical Paper No. 860606*.

[11] Wang, P.C., Corten, H.T., and Lawrence, F.V. (1985) A Fatigue Life Prediction Method for Tensile-Shear Spot Welds, *SAE Technical Paper No. 850370*.

[12] Swellam, M.H. (1991) A Fatigue Design Parameter for Spot Welds*, Ph.D. Thesis*, The University of Illinois at Urbana-Champaign.

[13] Swellam, M.H., Kurath, P., and Lawrence, F.V., Jr. (1991) Electric-Potential-Drop Studies of Fatigue Crack Development in Tensile-Shear Spot Welds, ASTM STP 1122.

[14] Radaj, D. and Zhang, S. (1991) Simplified Formulae for Stress Intensity Factors of Spot Welds, *Eng. Frac. Mech.* 40, 233-236.

[15] Radaj, D. and Zhang, S. (1991) Stress Intensity Factors for Spot Welds Between Plates of Unequal Thickness, *Eng. Frac. Mech.* 39, 391-413.

[16] Radaj, D. and Zhang, S. (1992) Stress Intensity Factors for Spot Welds Between Plates of Dissimilar Materials, *Eng. Frac. Mech.* 42, 407-426.

[17] Rupp, A., Storzel, K., and Grubisic, V. (1995) Computer Aided Dimensioning of Spot-Welded Automotive Structures, *SAE Technical Paper No. 950711*.

[18] Sheppard, S.D. (1996) Further Refinement of a Methodology for Fatigue Life Estimation in Resistance Spot Weld Connections *Advances in Fatigue Lifetime Prediction Techniques: 3rd Volume,* ASTM STP 1292, American Society for Testing and Materials, Philadelphia, 265-282.

[19] Zhang, S. (2004) A Simplified Spot Weld Model for Finite Element Analysis, *SAE Technical Paper No. 2004-01-0818*.

[20] Kang, H. (2005) A Fatigue Damage Parameter of Spot Welded Joints Under Proportional Loading," *Int. J. Auto. Tech.* 6, 285-291.

[21] Kang, H., Dong, P., and Hong, J. (2007), Fatigue Analysis of Spot Welds Using The Mesh-Insensitive Structural Stress Method, *Int. J. Fatigue* 29, 1546-1553.

[22] Kang, H. and Barkey, M. E. (1999) Fatigue Life Estimation of Resistance Spot-Welded Joints Using an Interpolation/Extrapolation Technique, *Int. J. Fatigue* 21, 769-777.